Research Article

# Improving Anaerobic Co-Digestion Performance using Granular Activated Carbon for Enhanced Methane Production: A Case Study of Food Waste and Tofu Wastewater

Farida Hanum*
Department of Chemical Engineering, Faculty of Engineering, Universitas Sumatera Utara, Medan, Indonesia
Department of Applied Chemistry and Life Science, Toyohashi University of Technology, Toyohashi, Japan

Irvan Irvan, Bambang Trisakti, Rivaldi Sidabutar, Mhd Reza Kurniawan Lubis, Handerson Simanjuntak, Michael Michael and Thiodorus Marvin Tjandra
Department of Chemical Engineering, Faculty of Engineering, Universitas Sumatera Utara, Medan, Indonesia

Qiyam Maulana Binu Soesanto, Hirotsugu Kamahara and Hiroyuki Daimon
Department of Applied Chemistry and Life Science, Toyohashi University of Technology, Toyohashi, Japan

* Corresponding author. E-mail: faridahanum@usu.ac.id DOI: 10.14416/j.asep.2026.02.009
Received: 26 September 2025; Revised: 27 November 2025; Accepted: 22 December 2025; Published online: 23 February 2026


**Abstract**
The rapid depletion of conventional energy resources and global population growth have intensified the need for sustainable alternative energy sources, with biogas technology emerging as a promising solution. This study investigated co-digestion of food waste (FW) and tofu wastewater (TWW) for methane production and evaluated the effect of granular activated carbon (GAC) on process performance. Among FW:TWW ratios tested (1:2, 1:3, 1:4), the 1:3 mixture achieved the highest performance, with peak daily methane production of 124.04 ± 0.83 mL/gVS, cumulative methane yield of 278.53 ± 1.08 mL/gVS, and COD removal of 77.78 ± 0.31%. Supplementing the 1:3 mixture with 10 g/L GAC further improved methane generation, increasing peak daily methane production by 21.42 ± 0.56%, VS degradation by 6.84 ± 0.40%, and COD removal by 15.56 ± 0.77% relative to the control. Enhanced performance is attributed to improved microbial activity via direct interspecies electron transfer (DIET) and biofilm development on GAC surfaces. SEM confirmed the presence of biofilms on post-digestion GAC. BET analysis indicated mesoporous characteristics suitable for microbial colonization (type IV isotherms with H2-type hysteresis loops), with a specific surface area of 803.2 $m^2/g$, pore volume of 0.583 cc/g, and mean pore diameter of 2.907 nm. These findings demonstrate that GAC-assisted co-digestion can strengthen methane productivity and organic removal, supporting broader advancement of sustainable waste-to-energy strategies.

**Keywords**: Anaerobic co-digestion, Food waste, Granular activated carbon, Methane production, Tofu wastewater

## 1 Introduction

The rapid depletion of conventional energy resources, coupled with exponential global population growth, has intensified the urgent need for developing sustainable alternative energy sources [1]. The global scientific community has increasingly recognized the potential of renewable energy alternatives in addressing this challenge. Biogas technology has emerged as a particularly promising alternative to address the mounting global energy crisis. The production and utilization of methane–rich biogas offer multiple environmental benefits, including the mitigation of odorous emissions and reduction of greenhouse gas releases into the atmosphere, thereby contributing to improved air quality [2].

The feedstock for biogas production includes a diverse range of organic materials, including agricultural residues, animal manure, food waste, and energy crops. While feedstock availability exhibits

significant spatiotemporal variation, agricultural regions show particularly promising potential due to their high organic waste generation rates [3]. Among these various feedstock options, food waste (FW) represents a promising feedstock for methane production due to its high carbon to nitrogen (C:N) ratio (14–37) and high substrate concentration (chemical oxygen demand (COD) (19–346 g/L) and carbohydrate content (25.5–143 g/L)) [4], [5]. Currently, FW management in developing countries primarily relies on landfill disposal, with thermal treatment and biological processing as alternative methods. While landfilling remains the predominant disposal method, particularly in developing nations, this practice raises environmental concerns and overlooks FW's potential as a renewable energy source. The substantial biodegradable organic matter in food waste makes it an excellent candidate for methane generation through anaerobic digestion, particularly due to its rich composition of readily degradable carbohydrates that can be efficiently converted to biogas by anaerobic microorganisms [6].

Despite its promising characteristics, FW alone presents limitations as a feedstock for efficient methane production. Its high biodegradability leads to rapid formation and accumulation of volatile fatty acids (VFAs), which subsequently lowers the pH, resulting in the inhibition of methanogens and eventual digester failure [7]. The co–digestion with tofu wastewater (TWW) could address these limitations by providing alkalinity and buffering capacity to maintain pH stability. Additionally, TWW's characteristics complement FW's composition in several key ways. While TWW has a lower C:N ratio (13) and COD (4 g/L), its high protein content (2–9 g/L) addresses the protein deficiency of carbohydrate-rich FW, creating a more nutritionally complete substrate mixture for microbial growth, potentially leading to improved process stability and enhanced methane yields [8]–[10].

Anaerobic digestion is an environmentally friendly biotechnological process widely used to treat various organic waste materials while reducing waste generation and producing biomethane as a renewable energy source [11]. However, despite the validity of the anaerobic digestion process, it is difficult to maintain the anaerobic reactor's stability because of the instability of pH, the accumulation of toxic compounds, which inhibit the growth of microorganisms, and other important factors [12]. Additionally, when treating mixed industrial waste feedstocks, biogas production often fails to reach its maximum potential due to mass transfer limitations caused by long–chain fatty acids (LCFAs) present in the raw materials. These LCFAs can significantly impair the process efficiency if not properly managed. One promising solution to address this challenge is the incorporation of granular activated carbon (GAC), which serves as a conductive material that facilitates direct interspecies electron transfer (DIET) between syntrophic bacteria and methanogens [13]. The electrical conductivity of GAC, stemming from its highly ordered carbon structure and extensive surface area, enables it to function as an electron conduit within the anaerobic digestion matrix [14]. The conductive properties of GAC enable electron flow between microbial species without the need for intermediate hydrogen or formate production, thereby accelerating the conversion of organic acids to methane [15], [16]. This mechanism not only effectively degrades LCFAs into short–chain VFAs but also enhances the syntrophic oxidation of these intermediates [17]. The implementation of GAC has shown considerable improvements in both the hydrolysis–acidification and methanogenesis stages of the anaerobic digestion process [18]. Previous research has demonstrated GAC's effectiveness in enhancing methane production across different substrates. Notable improvements include a 10.6% increase in pig manure [19], a 13.7% increase in beetroot pulp and dried wheat substrates [20], and a significant 22.1% increase in poultry manure [11].

Beyond GAC, various conductive materials have been investigated for their potential to facilitate DIET and enhance anaerobic digestion performance. These include biochar, carbon nanotubes, and graphene [21]. Biochar, for instance, has demonstrated methane yield improvements through its porous structure and surface functional groups, though its conductivity is generally lower than that of GAC [22]. Carbon nanotubes and graphene, while exhibiting superior electrical conductivity compared to GAC, present challenges related to high material costs, potential toxicity concerns at elevated concentrations, and difficulties in recovery and reuse in full–scale applications [23], [24]. In the context of this study, GAC was selected as the conductive additive due to its remarkable adsorbing capacity, high mechanical strength, excellent chemical stability, and economic feasibility [13].

Figure 1 depicts the anaerobic co–digestion process of food waste and tofu wastewater with GAC supplementation developed in this study. This study addresses a critical research gap by investigating the

optimal mixing ratio of FW and TWW as feedstocks for biogas production, with particular emphasis on the novel incorporation of GAC to enhance the anaerobic digestion process. The addition of GAC represents an innovative approach to improving substrate degradation and methane production in co–digestion systems. This integrated approach not only advances the understanding of how GAC influences anaerobic digestion performance but also sets the foundation for future research in waste–to–energy applications and their practical implementation in industrial settings.

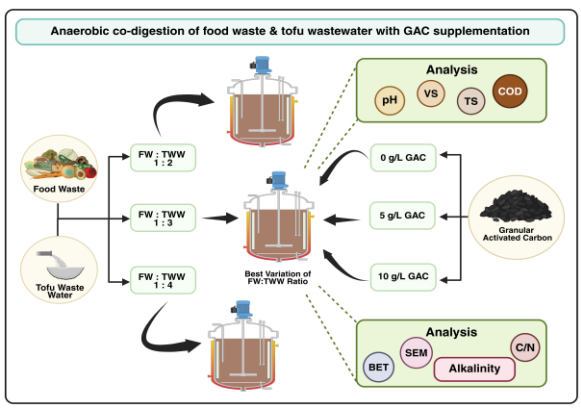


**Figure 1**: Schematic diagram of anaerobic co–digestion process of food waste and tofu wastewater with GAC supplementation developed in this study.

## 2 Materials and Methods

### 2.1 *Materials*

Fresh cow manure as inoculum was obtained through an established agreement with a local farm in Medan, Indonesia and undergoes anaerobic digestion (mesophilic plant, 1 $m^3$ capacity) pretreatment at the Ecology Laboratory, Universitas Sumatera Utara, Indonesia. Food waste (FW) and tofu wastewater (TWW) were locally sourced as primary substrates. Ultra–pure water ($H_2O$) was employed for sample preparation and apparatus cleaning. All chemical analyses utilized analytical–grade reagents. Hydrochloric acid (HCl, 37%) was procured from Merck KGaA® (Darmstadt, Germany) for alkalinity determinations. COD analysis employed the following analytical–grade reagents from Sigma–Aldrich (St. Louis, MO, USA): sulfuric acid ($H_2SO_4$, 98%), mercury(II) sulfate ($HgSO_4$, ≥99%), potassium dichromate ($K_2Cr_2O_7$, ≥99.9%), silver sulfate ($Ag_2SO_4$, ≥99.9%, ferroin indicator solution (0.025 M), and ferrous ammonium sulfate hexahydrate ($Fe(NH_4)_2(SO_4)_2 \cdot 6H_2O$, ≥98%). Carbon–to–nitrogen (C/N) ratio determinations utilized additional analytical–grade sodium hydroxide (NaOH, ≥99%) from Sigma–Aldrich.

### 2.2 *Methods*

#### *2.2.1 Preparation of Inoculum and Substrate*

Inoculum preparation for anaerobic digestion begins with cow manure obtained from an anaerobic fermentor. The initial step involves mixing cow manure with water at a biomass–to–volume ratio of 1:1, followed by thorough homogenization. The system is maintained at a pH range of 6.5–7.5 at room temperature for 14 days to allow microbes to adapt to environmental conditions, not to immediately produce main biogas, but to create optimal conditions for the subsequent methanogenic fermentation process until methane and characteristic fermentation compounds are observed. The inoculum was subsequently introduced at a proportion equivalent to one-third of the reactor's working volume, corresponding to approximately 2 L per fermentor. The substrate consists of FW collected from local restaurants and TWW obtained from a manufacturing facility in Medan, Indonesia, both filtered through a 2 mm sieve to remove coarse particles. FW is mechanically reduced in size through high–shear mixing before being homogenized with TWW at volumetric ratios of 1:2, 1:3, and 1:4. Preliminary assessments excluded the 1:1 ratio owing to the high acidity of FW (pH ≈ 4.86, later reported in Table 1), which would substantially depress the initial pH of the substrate mixture, thereby elevating the risk of process inhibition during the early stages of fermentation. Consequently, ratios spanning 1:2–1:4 were selected to ensure adequate dilution and buffering capacity via TWW addition, maintain pH within proximity to the optimal range for methanogenic activity, and establish a more balanced C/N ratio conducive to enhanced microbial metabolic performance [25], [26]. Following substrate homogenization, the inoculum is introduced at a substrate–to–inoculum ratio of 2:1 (v/v). Subsequently, the resultant mixture is transferred to the fermentor for a 21–day anaerobic digestion period. The substrate combination exhibiting the highest methane yield is subsequently evaluated with GAC supplementation of 0 g/L (control), 5 g/L, and 10 g/L. Daily quantification encompasses biogas production, including volumetric yield and methane content.

Concurrent characterization of the digestate includes analysis of total solids (TS), volatile solids (VS), pH, alkalinity, COD, and carbon–to–nitrogen (C/N) ratio. All feedstock characterization methodologies conform to American Public Health Association (APHA) standardized methodologies.

### *2.2.2 Fermentor operation*

The anaerobic digestion process was conducted using an MBF–1000 ME microbial fermentor (Eyela World, Tokyo, Japan) configured with a 7 L working volume. Temperature was maintained at 45 ± 1 °C using a thermostatic water jacket system, while continuous agitation at 60 rpm was provided by dual stainless–steel impellers. Prior to reaction initiation, the system underwent nitrogen gas sparging for 5 minutes to ensure complete oxygen displacement from the system. Biogas production was quantified daily using a calibrated wet gas meter (Model W–NK–1, Shinagawa Corp., Tokyo, Japan). To ensure accurate methane quantification, hydrogen sulfide ($H_2S$) was removed from the biogas stream via an iron oxide scrubbing system integrated into the gas pipeline system.

### *2.2.3 Quantification of methane content*

The methane content was quantified indirectly by measuring the $CO_2$ concentration using a GASTEC 2HT detector tube (GASTEC Corporation, Japan). Given that biogas primarily consists of methane and carbon dioxide, with other gases present in negligible quantities, the methane percentage was calculated by subtracting the measured $CO_2$ percentage from 100% [27]. Because $H_2S$ had been removed from the biogas stream via an iron oxide scrubbing system (Section 2.2.2), this method assumes the remaining fraction is predominantly methane, thereby neglecting the concentrations of trace gases (e.g., $H_2$ and $N_2$).

### *2.2.4 Quantification of C/N*

The carbon–to–nitrogen (C/N) ratio of the samples was quantified by determining the concentrations of organic carbon (C–organic) and organic nitrogen (N–organic) using spectrophotometric and volumetric methods, respectively. Organic carbon was measured via spectrophotometry following oxidation of the sample using an appropriate oxidizing agent, after which the absorbance was recorded at a specific wavelength corresponding to the formed chromophore. Calibration curves prepared from standard carbon solutions were used to calculate the C-organic concentration. Organic nitrogen was determined through volumetric analysis based on the digestion of nitrogenous compounds into ammonium ions, followed by distillation and titration with standardized acid or base solutions. The titration volume required to reach the endpoint was used to compute the N–organic content according to established analytical formulas. The C/N ratio was subsequently obtained by dividing the measured organic carbon concentration by the organic nitrogen concentration. This combined spectrophotometric–volumetric approach provides reliable and reproducible quantification of the C/N ratio for characterizing the biochemical composition of the samples.

### *2.2.5 Characteristics of Food Waste/Tofu Wastewater Substrate*

The quantification of total solids (TS) and volatile solids (VS) was conducted following APHA Standard Methods 2540B and 2540E, respectively [28], [29]. For TS determination, porcelain crucibles were initially prepared by heating at 550 °C for 1 hour in a muffle furnace, followed by cooling in a desiccator to room temperature, and their weights were recorded as $W_1$. Subsequently, a homogenized sample was transferred into the pre–weighed crucible and weighed ($W_2$), then subjected to drying at 105 °C in an oven for 24 h until achieving constant weight. Following desiccation and cooling to ambient temperature, the crucible containing the dried sample was weighed again ($W_3$). The TS content was calculated using Equation (1):

$$\text{TS (\%)} = \frac{W_3 - W_1}{W_2 - W_1} \times 100\% \quad (1)$$

For VS analysis, the dried residue from the TS determination was further combusted in a muffle furnace at 550 °C for 1.5 ho to volatilize and oxidize all organic matter to $CO_2$, leaving only the ash residue. After cooling in a desiccator to room temperature, the crucible containing the ash was weighed ($W_4$). The VS content was then further calculated as Equation (2):

$$\text{VS (\%)} = \frac{W_3 - W_4}{W_3 - W_1} \times 100\% \quad (2)$$

where $W_1$ is the weight of the empty crucible (g), $W_2$ is the weight of the crucible plus wet sample (g), $W_3$

is the weight of the crucible plus dried sample (g), and $W_4$ represents the weight of the crucible plus ash (g). This sequential analytical procedure enables the comprehensive characterization of both total and volatile solid content in the digestate sample matrix.

The digestate's pH was quantified using a pH meter (HI 5221, Hanna Instruments, USA) coupled with a HI 1131B glass electrode. Alkalinity determination was conducted via acid–base titration using standardized 0.1 N HCl. The protocol involved transferring 5 mL of digestate into a glass beaker and subsequently diluting it to 80 mL with deionized water. The solution was homogenized using a magnetic stirrer, and the pH probe was immersed in the mixture. Following the stabilized stirring process, the sample underwent titration with 0.1 N HCl until reaching the endpoint pH of 4.8 ± 0.02. The total alkalinity was subsequently derived using the following Equation (3) as follows [30]:

$$\text{Alkalinity (mg/L)} = \frac{V_{HCl} \times N_{HCl} \times 1{,}000 \times 50}{V_{sample}} \quad (3)$$

where $V_{HCl}$ is the volume of 0.1 N HCl used for titration (mL), $N_{HCl}$ is the normality of HCl (N), 50,000 is the equivalent weight of $CaCO_3$ (mg), and $V_{sample}$ is the volume of the sample (mL).

The COD was quantified as total (unfiltered) in accordance with the standardized method in APHA 5220B [31]. The analytical procedure involved a homogenized sample in a sealed reflux apparatus using potassium dichromate ($K_2Cr_2O_7$) as the primary oxidizing agent, with the reaction medium consisting of concentrated sulfuric acid ($H_2SO_4$) catalyzed by silver sulfate ($Ag_2SO_4$). Mercuric sulfate ($HgSO_4$) was incorporated to eliminate potential chloride interference. The oxidation process was conducted in reflux vessels at 150 °C i.e. a water bath, for 2 hours. The reaction mixture was cooled to ambient temperature prior to quantitative analysis. The post–oxidation $K_2Cr_2O_7$ underwent volumetric titration against standardized ferrous ammonium sulfate (FAS, $Fe(NH_4)_2(SO_4)_2$) solution with ferroin as the redox indicator. The titration endpoint was characterized by a distinctive color transition from green to reddish–brown. The COD concentration was subsequently calculated using Equation (4) [32]:

$$\text{COD (mg/L)} = \frac{(A - B) \times M \times 8{,}000}{V_{sample}} \quad (4)$$

where A is the volume of FAS consumed by blank (mL), B is the volume of FAS consumed by sample (mL), M is the molarity of FAS solution (M), and V is the sample volume (mL). The factor 8,000 signifies the milligram equivalent weight of oxygen per equivalent (mg $O_2$/eq), derived from the molecular weight of oxygen (32,000 mg/mol) divided by its electron equivalence value (4 eq/mol), resulting in the expression of COD in standard units of mg $O_2$/L.

### *2.2.6 Characterization of granular activated carbon*

Surface area and pore characteristics of the GAC were analyzed using the Quantachrome NOVA 2200E system (Quantachrome Corp., Florida, USA) at −196 °C with the relative pressure ($p/p_0$) range: 0.001–0.99. The Brunauer–Emmett–Teller (BET) equation was used to obtain the surface area, while the density functional theory (DFT) was utilized to obtain pore size distribution. The analysis involved taking approximately 0.4 g of the GAC sample and degassing at 300 °C for 3 h. The BET surface area and pore size distribution were then determined through nitrogen adsorption-desorption isotherms conducted at 77 K [33].

Micromorphological characterization of the granular activated carbon (GAC) surface was conducted via scanning electron microscope (JSM–35 CF, JEOL Ltd., Tokyo, Japan) at magnifications of 500× to serve as complementary analysis to the BET surface area measurements. The acquired micrographs were subsequently processed and analyzed using Image–Pro Plus (IPP) software (Media Cybernetics, Maryland, USA) to extract relevant structural information.

### *2.2.7 Statistical analysis*

All experiments were conducted in triplicate (n = 3). Results are expressed as mean ± standard deviation (SD). Statistical comparisons were performed using two-way analysis of variance (ANOVA), with statistical significance established at a threshold of *p*-value < 0.05 (Origin 2025b, OriginLab Corp., Massachusetts, USA).

## 3 Result and Discussion

### 3.1 *Characterization of feedstocks*

All feedstock characterizations that conform to standardized methodologies are detailed in Table 1.

These physicochemical characteristics demonstrate the significant methanogenic potential of the inoculum, TW, and FW as anaerobic digestion substrates.

The TSS and VSS values indicate substantial particulate matter content, with VSS/TSS ratios of approximately 0.928, 1.000, and 0.944 for inoculum, FW, and TWW, respectively. These high ratios suggest that the majority of suspended solids consist of organic matter, which is particularly favorable for biological treatment processes. The VS/TS ratios of 0.933 (inoculum), 0.750 (FW), and 0.942 (TWW) further corroborate the predominance of biodegradable organic components in these feedstocks.

The alkalinity values demonstrate significant variations among the feedstocks, with the inoculum exhibiting the highest buffering capacity at 2,100 mg/L, followed by TWW at 1,300 mg/L. The notably lower alkalinity of FW (100 mg/L) coupled with its acidic pH of 4.86 suggests potential susceptibility to pH fluctuations during digestion, which may necessitate alkalinity supplementation by excessive incorporation of TWW (pH 7.02) during the anaerobic treatment process. TWW exhibits the highest COD concentration at 152,000 mg/L, indicating a substantial organic loading potential. This elevated COD content, combined with its favorable pH and moderate alkalinity, suggests that TWW could serve as an excellent substrate for anaerobic digestion, though careful organic loading rate management would be crucial to prevent system overload.

Quantitatively, the observed COD values substantially exceed those reported for comparable organic substrates, such as tempeh wastewater at 22,500 mg/L [34]. COD serves as a critical parameter for microbial metabolism and growth [35], while elevated VS content indicates substantial biodegradable organic matter available for methanogenic conversion [36]. The VS concentrations markedly surpass those documented for tempeh wastewater at 5,810 mg/L [37]. Furthermore, the pH values are more favorable than those of tempeh wastewater, which exhibits an acidic pH of 4.5 [34]. Notably, FW demonstrates pH characteristics within the optimal range of 6.8–7.2 for methanogenesis [38], thus suggesting inherent compatibility with anaerobic digestion processes.

### 3.2 *Preliminary food waste: Tofu wastewater ratio analysis pre-granular activated carbon incorporation*

The study evaluated several key parameters, including daily and cumulative methane yields (normalized to fermentor volume, L methane/L fermentor), TS, VS, pH, alkalinity, COD, and carbon-to-nitrogen (C/N) ratio. Daily methane production was collected using a 7 L working volume fermentor. Figure 2(a) shows the daily methane production for each composition. Initial methane production was observed on day 1 across all variations, with a 1:3 ratio (FW:TWW) showing the highest output of 18.33 ± 0.62 mL/gVS, followed by 1:4 and 1:2 at 15.63 ± 0.42 mL/gVS and 9.42 ± 0.26 mL/gVS, respectively. After a brief decline between days 2–4, methane production increased significantly on day 5, with a 1:3 mixture achieving a peak production of 124.04 ± 0.83 mL/gVS on day 10. This performance notably outperformed the smallest ratio of 1:2, which reached only 35.25 ± 0.18 mL/gVS at its peak on day 11, representing a substantial 251.89 ± 0.79% difference in production capacity ($p < 0.01$, n = 3).

**Table 1**: Physicochemical characteristics of anaerobic digestion feedstocks.

| Parameters | UoM[a] | Inoculum | FW | TWW | Method/Instrument |
|---|---|---|---|---|---|
| TS[b] | mg/L | 60,000 | 8,000 | 70,000 | APHA 2540B |
| VS[c] | mg/L | 56,000 | 6,000 | 66,000 | APHA 2540E |
| TSS[d] | mg/L | 28,000 | 4,000 | 36,000 | APHA 2540D |
| VSS[e] | mg/L | 26,000 | 4,000 | 34,000 | APHA 2540E |
| pH[f] | - | 7.15 | 4.86 | 7.02 | pH Meter |
| Alkalinity | mg/L | 2,100 | 100 | 1,300 | Titration |
| COD[g] | mg/L | 48,000 | 56,000 | 152,000 | APHA 5220B |

*[a]UoM = Unit of measurement, [b]TS = Total solids, [c]VS = Volatile solids, [d]TSS = Total suspended solids, [e]VSS = Volatile suspended solids, [f]pH = Potential of hydrogen, [g]COD = Chemical Oxygen Demand.*

Methane production subsequently decreased sharply until day 15 before gradually ceasing by day 20. For comparison, a previous study by Orangun *et. al*., [39] reported a lower production level of 42 mL/gVS on day 4 by using goat manure and food waste at a 3:2 ratio. However, the combination with durian shell waste by Muenmee *et. al*., [40] successfully generated 60.63 mL/gVS by day 26 in a small–scale 125 mL anaerobic digester. This study achieved peak methane production on day 10, earlier than previous studies

using domestic waste, attributable to the more readily degradable organic content in this study's substrate combination. The cumulative methane production trends are shown in Figure 2(b).

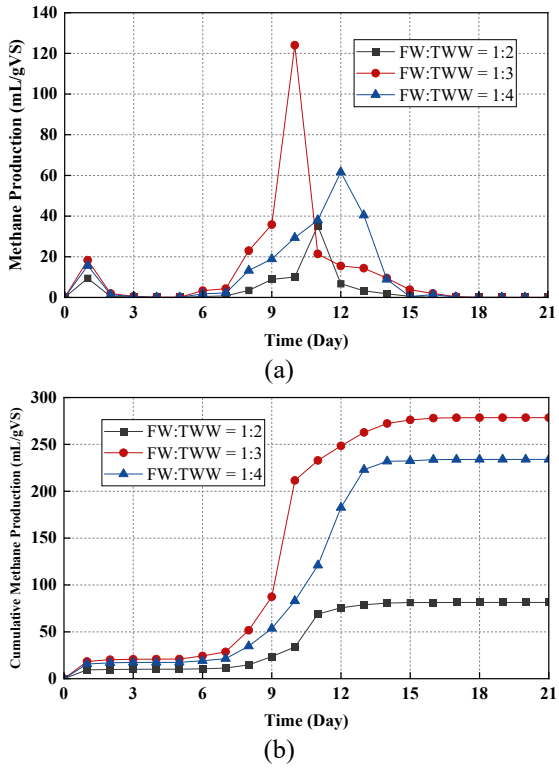


**Figure 2**: Methane production profiles in fermentors: (a) Daily methane yield, (b) Normalized cumulative methane production.

The progression of methane generation followed a distinct pattern: initial slow accumulation (days 1–7), followed by significant acceleration (days 7–12), before reaching a stagnation point from day 18 onwards. The ratio of 1:3 demonstrated superior performance with a total cumulative methane production of 278.53 ± 1.08 mL/gVS, significantly outperforming 1:2 ratio for methane production of 81.34 ± 0.48 mL/gVS by 242.43 ± 0.98% ($p$-value <0.05, n = 3). These cumulative production values represent a marked improvement over the performance by Orangun *et. al.,* [39], whose investigation yielded 168.5 mL/gVS at the four–day interval using a mixture consisting of goat manure and food waste at a 3:2 ratio. The higher production ratio obtained in this study can be attributed to the enhanced organic content of tofu wastewater. However, biogas quality analysis revealed varying $CH_4$ content across variations (1:2 of 51–57%, 1:3 of 53–62%, and 1:4 of 50–54%). The 1:3 ratio demonstrated both the highest methane production volume and the highest methane content, indicating this ratio provides optimal conditions for both methane quantity and quality. These findings align with Johnravindar *et. al.,* [41], who reported $CH_4$ content of 30–55% in food waste and waste activated sludge mixtures, and Muzyka *et. al.,* [42], who discovered $CH_4$ content of 53–58% in agriculture and organic fraction of municipal solid waste digesters.

Moderate mixing variation of 1:3 demonstrated superior performance across all parameters tested. As illustrated in Figure 3(a) and (b), this ratio also achieved the highest reduction in both TS and VS, with degradation rates of 49.18 ± 0.34% and 65.52 ± 0.97%, respectively. These findings are comparable to those reported by Rattanapan *et. al.,* [28], who observed TS degradation of 37.74% and VS degradation of 69.71% during a 25–day anaerobic fermentation process using food waste and domestic wastewater.

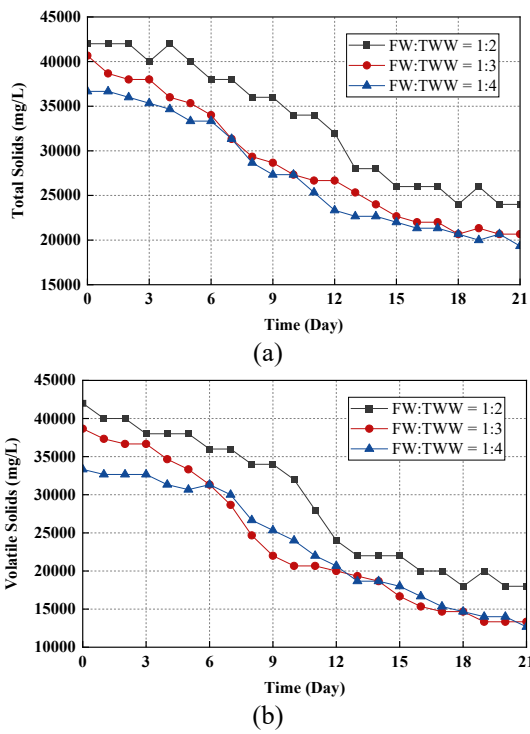


**Figure 3**: Solids degradation profiles in reactors: (a) TS concentration, (b) VS reduction dynamics.

A significant pH decline can be observed in Figure 4(a), during the initial four days of digestion,

with values dropping to 6.32–6.43, corresponding to active hydrolysis and acidogenesis phases [43]. The period of lowest methane production coincided with pH values between 6.39–6.72, occurring between days 2 and 5. Subsequently, the system showed recovery after day 5, marked by the conversion of VFAs (butyric and propionic acids) to acetic acid [44]. This acetogenic phase was followed by methanogenesis, during which the conversion of acetic acid to methane resulted in a gradual pH increase to 6.72–7.95, reflecting the consumption of acidic compounds [43]. The highest pH range, 7.19–7.46, occurred between days 10 and 12, coinciding with peak methane production. This pH range represents optimal conditions for methanogenic bacteria, which thrive in neutral to slightly alkaline environments, explaining the enhanced methane yields observed during this period. Afterwards, the pH rose further to 7.86–7.92, accompanied by a decrease in methane production up to day 21. This result aligns with the theory presented by Harirchi *et. al.,* [45], which states that the optimal pH for methane production is between 6.5 and 7.5.

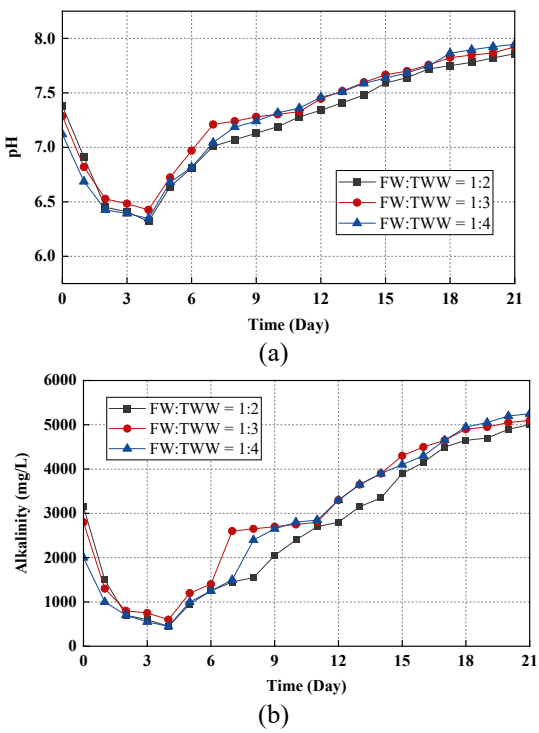


**Figure 4**: Process stability parameters in reactors: (a) Temporal pH fluctuation, (b) Alkalinity profile throughout the anaerobic digestion period.

Alkalinity represents the ability of raw materials to neutralize acids during anaerobic fermentation [46]. According to this study, alkalinity and pH are closely related. As shown in Figure 4(b), variations in alkalinity closely mirrored changes in pH values. The initial alkalinity values ranged from 2,000 to 3,150 mg/L, followed by a marked decrease that coincided with pH reduction until day 4, reaching minimum values of 450 to 600 mg/L. After that, alkalinity increases, reaching a range of 5,000 mg/L to 5,250 mg/L. The result demonstrated that the stability for digestion process is within an acceptable range across all variations.

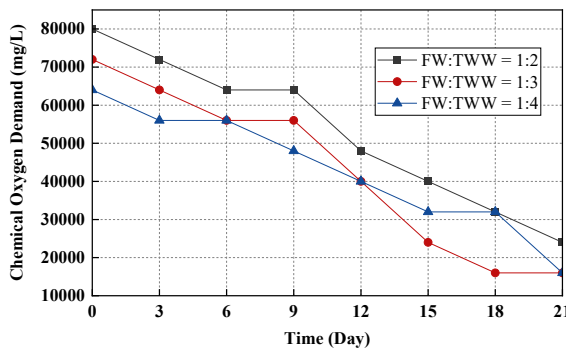


**Figure 5**: COD reduction profile in reactors during the anaerobic fermentation process.

For COD degradation, the ratio of 1:3 exhibited the highest degradation at 77.78 ± 0.31%, while the 1:2 ratio showed the lowest at 70 ± 0.48% (Figure 5). These results indicate a positive correlation between COD degradation and methane production, as COD serves as a measure of organic material. Therefore, a decrease in COD reflects a reduction in organic matter. Similar observations were reported by Ali *et. al.,* [47], where the highest COD degradation corresponded to the greatest methane production. Due to the superior performance of FW:TWW 1:3 ratio across all parameters, it will be selected as the feedstock composition for subsequent experiments involving different GAC concentrations.

### 3.3 *Performance analysis of selected food waste: Tofu wastewater ratio with granular activated carbon incorporation*

#### *3.3.1 Analysis of methane production and quality*

Following the incorporation of GAC into the system, methane formation was monitored across three GAC

concentrations (0, 5, and 10 g/L). As presented in Figure 6(a), initial methane formation was observed on day 1 across all variations, yielding 18.33 ± 0.62 mL/gVS, 22.61 ± 0.53 mL/gVS, and 23.03 ± 0.36 mL/gVS, respectively. This immediate production can be attributed to the active methanogenic bacteria present in the starter culture. Similar to the methane production pattern previously discussed, a temporary decline was observed during days 2–4, followed by a recovery from day 5, coinciding with the initiation of the hydrolysis process and subsequent acid production.

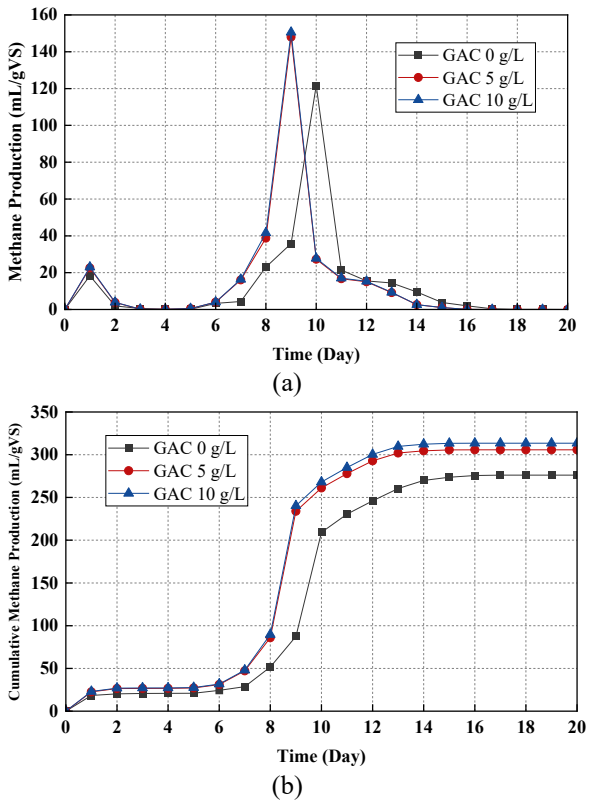


**Figure 6**: Effect of GAC supplementation on methane production: (a) Daily methane yield, (b) Normalized cumulative methane production under varying GAC concentrations.

A significant increase in methane production was observed after day 5, with the system incorporating 10 g/L GAC achieving peak daily production on day 9, one day earlier than the control system. The FW:TWW ratio of 1:3 supplemented with 10 g/L GAC yielded the highest peak methane production of 150.6 ± 0.52 mL/gVS, representing a statistically significant enhancement relative to both the 0 g/L and 5 g/L treatments ($p$-value < 0.01, n = 3). This increase is attributable to enhanced microbial activity supported by GAC, consistent with the relatively high biodegradable content of FW and the buffering capacity of TWW [48]. Compared to the 1:3 condition without GAC (124.04 ± 0.83 mL/gVS), the 21.42% improvement ($p$-value < 0.01, n = 3) indicates a genuine enhancement in conversion efficiency rather than merely reflecting substrate compositional differences. The FW fraction provides abundant biodegradable organics, while TWW offers a favorable C/N balance. However, only when supplemented with GAC did methane production increase significantly, thereby confirming that the observed improvement results from accelerated organic degradation and facilitated direct interspecies electron transfer (DIET) rather than intrinsic substrate quality alone [49], [50].

This observation aligns with the findings of Ziganshina *et. al.,* [11], who reported similar acceleration in peak daily methane production using chicken manure on day 5 and achieved a 20.19% increase in methane production with GAC addition. The enhanced performance can be attributed to GAC's ability to accelerate VFA formation [51]. Furthermore, GAC not only facilitates rapid VFA conversion to methane but also effectively adsorbs excess VFA, helping maintain optimal slurry conditions for methane formation. Following the peak at day 9, methane production decreased markedly until day 15, followed by a gradual decline until complete cessation at day 17. This production pattern indicates the completion of the anaerobic fermentation process, suggesting the exhaustion of substrate availability for methanogenic bacterial degradation.

The decline in daily methane production after reaching peak values corresponded with a stabilization in cumulative methane production, as presented in Figure 6(b). The cumulative methane production showed a gradual increase from days 1 to 7, followed by a significant rise until day 13. The process concluded at day 17 across all variations, with the 10 g/L GAC system completing fermentation three days earlier than the control system without GAC, supporting Jiang *et. al.,* [52] findings that GAC accelerates the anaerobic fermentation process. During the entirety of the anaerobic fermentation process, the highest cumulative methane volume was achieved with 10 g/L GAC, reaching 313.47 ± 1.68 mL/gVS, representing a 12.54 ± 0.24% increase compared to the system without GAC ($p$ < 0.01, n = 3). These results are comparable to those reported by

Ziganshina *et. al.,* [11], who observed an 11.63% increase in cumulative methane production using 10 g/L GAC with chicken manure substrate. The enhanced performance can be attributed to GAC's dual role in accelerating VFA formation and facilitating its conversion to methane, while simultaneously adsorbing excess VFA to maintain optimal slurry conditions [51].

### *3.3.2 Characterization of solid contents*

The volumetric increase in methane demonstrates a strong correlation with enhanced degradation rates of TS and VS. Capson-Tojo *et. al.,* [53] and Yang *et. al.,* [54] elucidated that GAC facilitates superior substrate degradation efficiency. The temporal progression of TS and VS degradation throughout the anaerobic fermentation process is respectively depicted in Figure 7(a) and (b).

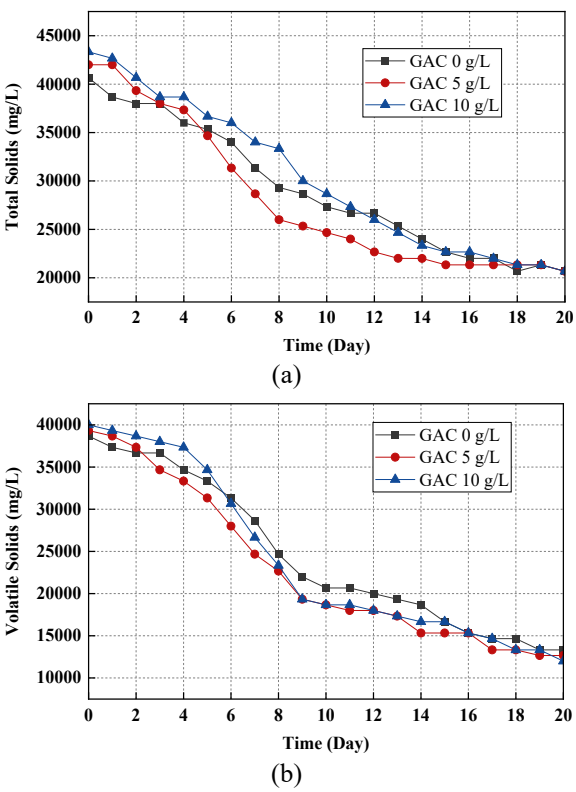


**Figure 7**: Impact of GAC on solids degradation: (a) TS temporal evolution, (b) VS degradation profiles under different GAC concentrations.

The anaerobic fermentation process exhibits a systematic decline in TS concentration. Initial TS concentrations ranged from 40,667 ± 113.04 mg/L to 43,333 ± 130.05 mg/L, ultimately diminishing to 20,667 ± 74.83 mg/L post-fermentation. The incorporation of 10 g/L GAC yielded remarkable TS degradation with a 52.31 ± 0.53% reduction. Conversely, the control condition (0 g/L GAC) achieved a comparatively modest 49.18 ± 0.34% TS degradation, thereby indicating that 10 g/L GAC implementation resulted in a 6.36 ± 0.48% enhancement in degradation efficiency. These findings align with those reported by Xiao *et. al.,* [55] wherein the introduction of 4.17 g/L GAC in a 1.2-liter fermentor for treating pig manure yielded a 5.3% improvement in TS degradation.

VS, representing the organic fraction of TS in the sample, exhibited improved degradation efficiency. The elevated VS degradation corresponds directly to increased methane production as attributable to the organic constituents' potential for methanogenic conversion [56]. A systematic decline in VS concentration throughout the fermentation period reflects their conversion to methane. Initial VS concentrations ranged from 38,667 ± 76.31 mg/L to 40,000 ± 161.86 mg/L, subsequently diminishing to 12,000 ± 36.13 to 13,333 ± 58.64 mg/L post-fermentation. Optimal VS degradation efficiency of 70 ± 0.85% was achieved with 10 g/L GAC incorporation, representing a 6.84 ± 0.40% enhancement compared to the control condition without GAC, which only achieved 65.52%. ($p$-value $< 0.05$, n = 3). Besides the statistical difference, a 5–10% improvement in VS removal typically indicates a more effective microbial conversion of organic matter into methane rather than remaining as residual solids. This result confirms that GAC addition promoted more efficient biodegradation, contributing to improved methane generation and overall process stability [30]. This augmented performance can be attributed to GAC's dual functionality: its capacity for VFA adsorption and its role as a substrate matrix for VS–degrading microorganisms [51]. The superior degradation rate observed at 10 g/L GAC concentration stems from its enhanced surface area, which facilitates optimal microbial colonization and subsequent VS degradation. Xiao *et. al.,* [41] reported that implementing 4.17 g/L of granular activated carbon yielded a relatively modest 2.3% improvement in volatile solids degradation efficiency. Our findings also surpass those of Ziganshina *et. al.,* [11], who observed a mere 2.35% enhancement in VS reduction when using 10 g/L GAC—a performance improvement that was statistically insignificant

compared to the lower incorporation of 5 g/L implemented in the same investigation. Since VS represents the methane–producing substrate while TS includes inert materials, this preferential VS enhancement directly explains the superior methane yields. The dose–dependent response and superior performance of 10 g/L GAC concentration demonstrate that adequate GAC surface area is critical for optimizing substrate–microorganism interactions throughout the digestion process.

### *3.3.3 Parameters of the digestion process stability*

pH condition is highly sensitive in the anaerobic fermentation process [57], because it affects the activity of microorganisms in degrading organic matter into methane [58]. pH changes during the anaerobic fermentation process in this study are shown in Figure 8.

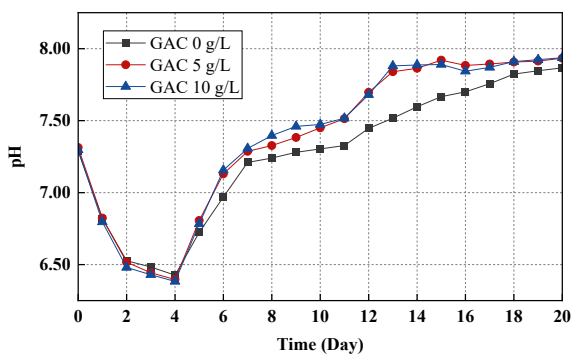


**Figure 8**: Temporal pH dynamics in GAC–supplemented anaerobic fermentation systems.

Compared to the process without GAC incorporation, the pH profiles exhibited distinct patterns during the anaerobic digestion process, with both processes showing initial decreases followed by recovery phases. During the first four days, pH decreased significantly to 6.38–6.43. This phenomenon is attributable to hydrolysis and acidogenesis processes [43], corresponding to the lowest methane production between days 2 to 5. While both processes showed pH recovery after day 5, the GAC–supplemented process demonstrated enhanced pH stabilization. This happens due to the metal elements and basic functional groups on the surface of the GAC that can improve the buffering capacity and stability of the digestion system, contributing to intermediate acid degradation [44]. By day 7, supplementation with 10 g/L GAC achieved a pH of 7.31 compared to 7.21 without the incorporation of GAC. This accelerated pH recovery in GAC–supplemented processes is attributed to enhanced VFA conversion rates [51], consistent with findings reported by Ziganshina *et. al.,* [20] on GAC's capacity to expedite pH stabilization. Changes in alkalinity during anaerobic fermentation in this study are shown in Figure 9.

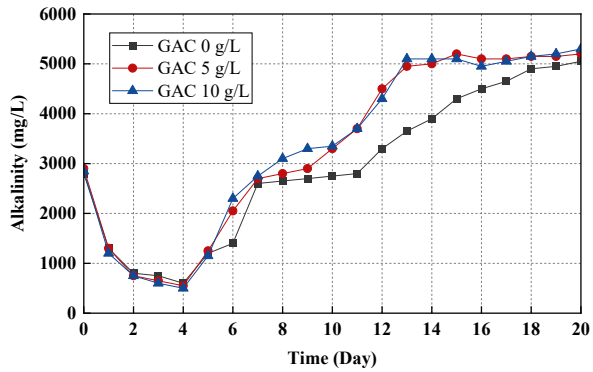


**Figure 9**: Alkalinity dynamics in GAC–supplemented anaerobic fermentation systems.

The alkalinity profiles demonstrated similar initial trends in both pre– and post–GAC processes, starting at 2,800-2,900 mg/L and declining linearly to 500–600 mg/L by day 4, coinciding with pH reduction. However, the recovery patterns diverged markedly after day 5, with GAC–supplemented reactors exhibiting enhanced buffering capacity. The presence of GAC accelerated alkalinity recovery through improved VFA conversion and adsorption mechanisms, ultimately achieving higher final alkalinity values of 5,300 mg/L compared to 5,050 mg/L in control reactors. This enhanced alkalinity recovery in GAC–supplemented systems indicates improved process stability and buffer capacity during the anaerobic digestion process.

### *3.3.4 Removal efficiency of organic matter*

COD is an indirect measure of the number of organic compounds, both biodegradable and non–biodegradable. It can be used to estimate the methane produced from biomass degradation. The decrease in COD values occurs due to hydrolysis, where microorganisms utilize organic materials as nutrients and convert them into simpler compounds [59]. COD analysis is conducted every three days to monitor organic matter degradation. During anaerobic

fermentation, a decrease in COD values is observed, reflecting the breakdown of substrates by bacteria [60]. In this study, the batch fermentor facilitated a decline in COD until it could no longer be converted into methane due to the microorganisms entering the death phase.

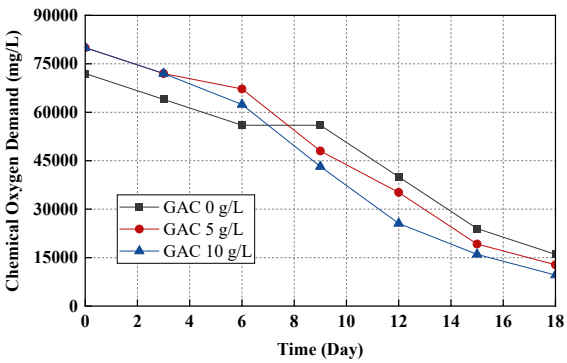


**Figure 10**: COD removal efficiency in GAC-supplemented anaerobic fermentation systems.

Figure 10 represents the COD degradation during the anaerobic fermentation process after GAC incorporation. During anaerobic fermentation, both processes demonstrated significant COD reduction, with GAC–supplemented reactors achieving lower endpoints from initial COD values of 72,000 ± 144.06 to 80,000 ± 151.77 mg/L, reduced to 9,600 ± 38.31 to 16,000 ± 72.21 mg/L by the end of the fermentation process. The GAC–supplemented system demonstrated the highest COD removal efficiency of 15.56 ± 0.77% in the 10 g/L system compared to the control. The improved performance with GAC incorporation aligns with previous studies, where Kalantzis *et. al.,* [61] reported a 16% efficiency increase with 5 g/L GAC addition, while Zaman *et. al.,* [62] achieved up to 9.84% COD removal with 5 g/L GAC, demonstrating the broad efficacy of GAC supplementation across different operational conditions.

### *3.3.5 Assessment of Carbon-to-Nitrogen (C/N) ratio*

The carbon–to–nitrogen (C/N) ratio significantly influences methanogenic activity during anaerobic fermentation. Table 2 presents the C/N ratios observed before and after the anaerobic fermentation process for a substrate mixture of FW and TTW (1:3 v/v) with varying concentrations of GAC.

The optimal C/N ratio for methanogenesis ranges between 15 to 30, as this range ensures sufficient nitrogen availability for microbial growth while preventing ammonia inhibition [63], [64]. As evidenced in Table 2, all initial variations exhibited C/N ratios within this optimal range. The significant decrease in C/N ratio observed in the control (without GAC incorporation) can be attributed to preferential carbon utilization by microorganisms during fermentation coupled with nitrogen accumulation [65]. Conversely, GAC-supplemented systems maintained relatively stable C/N ratios throughout the fermentation process. This stability is attributable to GAC's capacity to regulate organic carbon compounds by gradual release during fermentation [66]. Additionally, GAC's surface properties facilitate the immobilization of microbial communities [67]. This balanced nutrient availability, coupled with GAC presence, contributes to enhanced methane production through sustained methanogenic activity [68], [69].

**Table 2**: C/N ratio under optimum conditions of FW:TWW (1:3 v/v) substrate mixture before and after anaerobic fermentation under varying GAC concentrations.

| GAC Supplementation (g/L) | C/N Ratio | |
|---|---|---|
| | Initial | Final |
| 0 | 19.5 ± 0.12 | 12.5 ± 0.16 |
| 5 | 19.5 ± 0.12 | 14.5 ± 0.17 |
| 10 | 19.5 ± 0.12 | 16.0 ± 0.11 |

## 3.4 *Surface morphology analysis*

The surface morphology analysis was conducted using SEM at 500× magnification. The micrographs revealed the morphological transformations of GAC surfaces before and after anaerobic co–digestion treatment. The pristine GAC before usage (Figure 11(a)) exhibited a highly irregular surface with numerous sharp edges and crystalline structures. This complex topography creates an extensive network of micropores and mesopores distributed throughout the material, providing the high surface area characteristic of activated carbon [70]. In contrast, Figure 11(b) shows the microscopic morphology of the GAC after anaerobic co–digestion, where the surface appears significantly altered with a visible layer of biological

growth. The originally distinctive pore structures are partially obscured by what appears to be microbial biofilm formation, consistent with the findings of Gibert *et. al.,* [71] regarding biofilm development on GAC used for drinking water production. The observed morphological transformations suggest altered components interactions upon GAC utilization, affecting the overall digestion performance [72], [73]. Several key factors contributed to these morphological transformations. The high surface area and porous structure of GAC provided abundant attachment sites for microbial colonization, enabling syntrophic bacteria and methanogens to establish close physical proximity necessary for DIET. The electrical conductivity of GAC attracted electroactive microorganisms, promoting preferential biofilm development by these specific microbial communities [74].

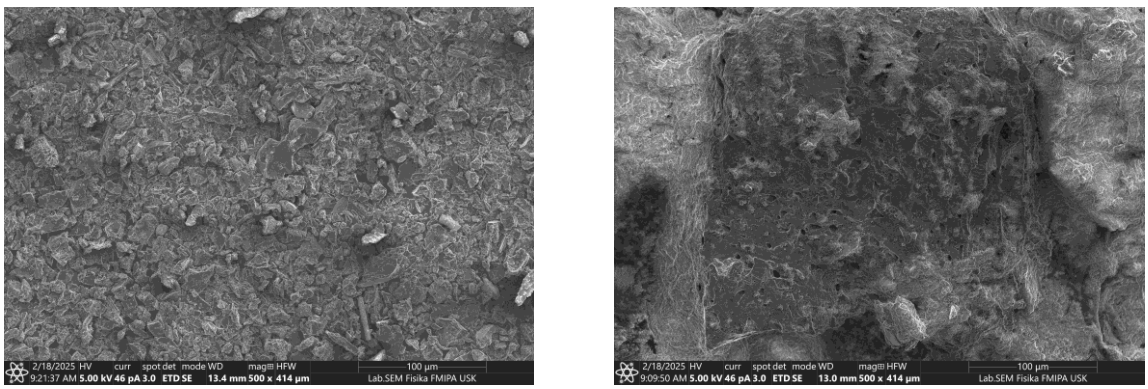


(a) (b)

**Figure 11**: Surface morphology transformation of GAC: (a) Prior to anaerobic co-digestion, (b) Recovered after anaerobic co–digestion.

### 3.5 *Surface area and porosity characteristics*

The surface area and porosity characterization were conducted using nitrogen gas physisorption techniques via the BET methodology, predicated on comprehensive nitrogen adsorption–ndesorption isothermal data. BET analysis represents a well–established analytical approach for determining the specific surface area of porous solid substrates. Figure 12 illustrates the linear nitrogen adsorption–desorption isotherms characteristic of the activated zeolite framework.

While the BET method is the most widely adopted technique for surface area determination, several alternative nitrogen adsorption approaches exist, each with distinct theoretical foundations and applications. The Langmuir method assumes monolayer adsorption on a homogeneous surface without lateral interactions between adsorbed molecules, providing surface area values typically 10–30% higher than BET due to its simplified assumptions. However, the Langmuir model is less suitable for heterogeneous materials like GAC, where multilayer adsorption occurs [75], [76]. The Barrett–Joyner–Halenda (BJH) method specifically calculates pore size distribution and mesopore volume from the desorption branch of the isotherm using the Kelvin equation, providing detailed information about pore geometry and distribution. However, the BJH method shows significant limitations when characterizing materials with pore dimensions close to the 2 nm micropore-mesopore boundary due to the breakdown of capillary condensation theory assumptions at small pore sizes, a concern directly applicable to GAC as it exhibits an average pore diameter of 2.907 nm [77], [78].

Figure 12 illustrates the nitrogen adsorption profile relative to $p/p_0$, revealing the GAC's adsorption–desorption isotherms characterized by an initial gradual increase followed by a steep ascent as $p/p_0$ approaches unity, accompanied by distinctive hysteresis loops. The adsorption curve exhibits a sharp initial uptake at very low relative pressures (below 0.05), followed by a steady, nearly linear increase in adsorbed volume as relative pressure increases from approximately 0.05 to 0.99, concluding in an accelerated uptake at high relative pressures (above 0.94). The pattern represents a Type IV isotherm typical of mesoporous materials, similar to that reported in other adsorbents [3], with complex pore

structures, likely featuring ink–bottle shaped pore openings or interconnected pore networks where pore blocking and percolation effects influence the desorption process [79]. The desorption curve follows a different path than the adsorption curve, displaying an H2–type hysteresis loop most prominent at higher relative pressures. The initial steep region indicates monolayer formation, the middle section represents multilayer adsorption, and the final upturn with H2 hysteresis suggests capillary condensation occurring within a network of mesopores with restricted entrances [80].

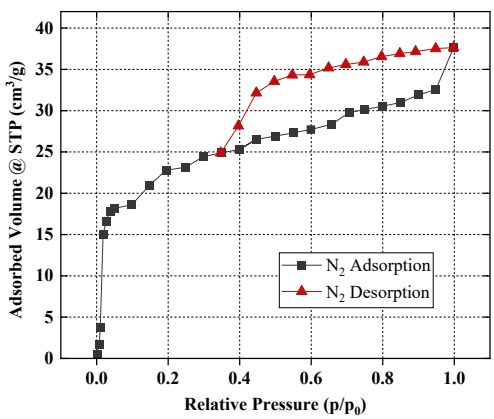


**Figure 12**: Adsorption–desorption isotherm of GAC.

**Table 3**: Pore characteristics of synthesized and commercial GAC.

| Materials | Surface Area ($m^2$/g) | Pore Volume (cc/g) | Pore Diameter (nm) |
|---|---|---|---|
| Current Study | 803.2 | 0.583 | 2.907 |
| Commercial GAC* | 900–1,300 | 0.5–1.0 | 2–50 |

*Source: Alibaba

In the BET analysis, characteristics of GAC include surface area, pore volume, and average pore diameter, which were characterized (as shown in Table 3), yielding values of 803.2 $m^2$/g, 0.583 cc/g, and 2.907 nm, respectively. The BET results indicate that the GAC has a relatively high surface area, though it falls at the lower end of the commercial GAC range (900–1,300 $m^2$/g). The pore volume of the synthesized GAC falls within the typical commercial range, suggesting adequate adsorption capacity. The average pore diameter of 2.907 nm indicates that the synthesized GAC contains predominantly micropores and small mesopores, positioning it at the lower end of the commercial GAC pore diameter range (2–50 nm). This approach demonstrates the potential of GAC in enhancing the anaerobic co–digestion of FW and TWW by providing attachment sites for microbial colonization and adsorbing inhibitory compounds [81], [82], which are crucial for commercial applications for improving methane production yields and process stability.

### 3.6 *Future prospects and practical implication*

Building on the promising outcomes of this study, several opportunities arise for further exploration of GAC in anaerobic co–digestion systems. Future research should extend to pilot– and full–scale trials to validate the effectiveness of GAC supplementation under continuous operational conditions. Particular attention should be given to evaluating dosages beyond the 10 g/L applied in this work, as higher concentrations may reveal performance thresholds, additional benefits, or potential inhibitory effects.

Long–term investigations are also needed to understand microbial community dynamics, biofilm stability, and overall process robustness when GAC is continually applied. In parallel, strategies for regeneration, reuse, or recycling of spent GAC must be developed to improve cost–effectiveness and minimize environmental impact. Furthermore, techno–economic assessments and life–cycle analyses will be critical to determine the feasibility of large–scale implementation across municipal, industrial, and agro–industrial contexts. Finally, integrating GAC supplementation into existing digester designs, whether through retrofitting or modular enhancements, offers a practical pathway for rapid adoption in established waste–to–energy facilities.

From a practical standpoint, this study confirms that GAC–assisted co–digestion enhances methane yield, accelerates digestion kinetics, and stabilizes process parameters, thereby offering a viable means of improving the efficiency of current biogas systems. By enabling the valorization of readily available residues such as FW and TWW, the approach contributes to renewable energy recovery while reducing environmental burdens associated with landfilling and greenhouse gas emissions. The straightforward integration of GAC into anaerobic digesters further supports industrial and municipal feasibility, particularly in regions with existing waste treatment infrastructure. Taken together, these prospects highlight the potential of GAC–assisted anaerobic digestion as a scalable and impactful waste–to–energy strategy that aligns with broader sustainability and climate action goals.

## 4 Conclusions

This study identified an FW:TWW ratio of 1:3 as the optimal co-digestion mixture, yielding the highest methane production and stable operating conditions. Supplementing this mixture with 10 g/L GAC further enhanced performance, resulting in a 21.42 ± 0.56% increase in peak methane production, methane content up to 61%, improved VS degradation (6.84 ± 0.40%), and greater COD removal (15.56 ± 0.77%) compared with the control. The addition of GAC also supported faster pH recovery and contributed to improved process stability. These enhancements are attributed to strengthened microbial interactions, likely facilitated by DIET and biofilm development on GAC surfaces. SEM confirmed biofilm presence on post-digestion GAC, while BET analysis indicated a high specific surface area conducive to microbial attachment. Overall, integrating GAC into FW:TWW co-digestion can improve methane productivity, accelerate process stabilization, and enhance organic matter degradation that reduces treatment time and improves overall feasibility of waste-to-energy systems. Further development should explore long-term reactor performance, GAC regeneration/reuse, and scale-up under continuous operation to validate practical application. Integration with industrial tofu and food-waste streams may offer a promising pathway toward more sustainable organic-waste management and renewable energy generation.

## Acknowledgments

This research received no specific grant from any funding agency in the public, commercial, or not-for-profit sectors.

## Author Contributions

F.H.: Conceptualization, Writing – review & editing. I.I.: Supervision, Validation. B.T.: Supervision, Validation. R.S.: Data curation, Formal analysis. M.R.K.L.: Data curation, Formal analysis, Methodology, Writing – original draft. H.S.: Methodology, Writing – original draft. M.M.: Project administration, Visualization. T.M.T.: Formal analysis, Writing – original draft. Q.M.B.S.: Conceptualization, Investigation, Writing – review & editing. H.K.: Methodology, Writing – review & editing. H.D.: Supervision, Validation. All authors have read and agreed to the published version of the manuscript.

## Conflicts of Interest

The authors declare no conflict of interest.

## References

[1] P. Nyamukamba, P. Mukumba, E. S. Chikukwa, and G. Makaka, "Biogas upgrading approaches with special focus on siloxane removal—A review," *Energies*, vol. 13, 2020, doi: 10.3390/en13226088.

[2] M. Shen et al., "A review on removal of siloxanes from biogas: With a special focus on volatile methylsiloxanes," *Environmental Science and Pollution Research*, vol. 25, pp. 30847–30862, 2018, doi: 10.1007/s11356-018-3000-4.

[3] R. Sidabutar et al., "Synergistic integration of zeolite engineering and fixed-bed column design for enhanced biogas upgrading: Adsorbent synthesis, $CO_2/CH_4$ separation kinetics, and regeneration assessment," *Separation and Purification Technology*, vol. 355, 2025, doi: 10.1016/j.seppur.2024.129772.

[4] M. M. Habashy, E. S. Ong, O. M. Abdeldayem, E. G. Al-Sakkari, and E. R. Rene, "Food waste: A promising source of sustainable biohydrogen fuel," *Trends in Biotechnology*, vol. 39, pp. 1274–1288, 2021, doi: 10.1016/j.tibtech.2021.04.001.

[5] O. P. Karthikeyan, E. Trably, S. Mehariya, N. Bernet, J. W. C. Wong, and H. Carrere, "Pretreatment of food waste for methane and hydrogen recovery: A review," *Bioresource Technology*, vol. 249, pp. 1025–1039, 2018, doi: 10.1016/j.biortech.2017.09.105.

[6] N. Ferronato and V. Torretta, "Waste mismanagement in developing countries: A review of global issues," *International Journal of Environmental Research and Public Health*, vol. 16, 2019, doi: 10.3390/ijerph16061060.

[7] U. Bista, B. Rayamajhi, B. Dhungana, and S. P. Lohani, "Biogas production by co-digestion of food waste with sewage sludge and poultry litter: A way towards sustainable waste-to-energy conversion," *Journal of Renewable Energy and Environment*, vol. 10, pp. 39–44, 2023, doi: 10.30501/jree.2022.333462.1342.

[8] R. N. Amalia et al., "Potensi limbah cair tahu sebagai pupuk organik cair di RT. 31 Kelurahan Lempake Kota Samarinda," *Jurnal Pengabdian Masyarakat Universitas Mulawarman*, vol. 1, pp. 36–41, 2022, doi: 10.32522/abdiku.v1i1.38.

[9] N. R. Mardiyah and Y. S. Purnomo, "Pemanfaatan unsur makro (NPK) limbah cair tahu untuk pembuatan pupuk cair secara aerobik," *Jurnal Envirotek*, vol. 9, no. 2, 2012, doi: 10.33005/envirotek.v9i2.967.

[10] Widyarani et al., "Distribution of protein fractions in tofu whey wastewater and its potential influence on anaerobic digestion," *IOP Conference Series: Earth and Environmental Science*, vol. 277, 2019, doi: 10.1088/1755-1315/277/1/012012.

[11] E. E. Ziganshina, S. S. Bulynina, and A. M. Ziganshin, "Impact of granular activated carbon on anaerobic process and microbial community structure during mesophilic and thermophilic anaerobic digestion of chicken manure," *Sustainability*, vol. 14, 2022, doi: 10.3390/su 14010447.

[12] B. Tonanzi et al., "Elucidating the key factors in semicontinuous anaerobic digestion of urban biowaste: The crucial role of sludge addition in process stability, microbial community enrichment and methane production," *Renewable Energy*, vol. 179, pp. 272–284, 2021, doi: 10.1016/j.renene.2021.07.049.

[13] L. Xiao et al., "Enhanced methane production by granular activated carbon: A review," *Fuel*, vol. 320, 2022, doi: 10.1016/j.fuel.2022.123903.

[14] B. Azad, L. Wu, H. Duan, and J. Qian, "Enhanced anaerobic digestion performance with carbon-based material additives towards sustainable energy production: A comprehensive review," *Journal of Cleaner Production*, vol. 525, 2025, doi: 10.1016/j.jclepro.2025.146616.

[15] M. Nabi et al., "A comprehensive review on the use of conductive materials to improve anaerobic digestion: Focusing on landfill leachate treatment," *Journal of Environmental Management*, vol. 309, 2022, doi: 10.1016/j.jenvman.2022. 114540.

[16] L. M. Ningsih et al., "The effect of pretreatment on VFA production from tofu and tempeh wastewater through anaerobic digestion batch," *SSRN Electronic Journal*, 2024, doi: 10.2139/ ssrn.5093687.

[17] S. Qian et al., "Research on methane-rich biogas production technology by anaerobic digestion under carbon neutrality: A review," *Sustainability*, vol. 17, no. 4, 2025, doi: 10.3390/ su17041425.

[18] Y. Liu et al., "Enhancing anaerobic digestion process with addition of conductive materials," *Chemosphere*, vol. 278, 2021, doi: 10.1016/ j.chemosphere.2021.130449.

[19] Y. Xiao et al., "Improved biogas production of dry anaerobic digestion of swine manure," *Bioresource Technology*, vol. 294, 2019, doi: 10.1016/j.biortech.2019.122188.

[20] E. E. Ziganshina, D. E. Belostotskiy, S. S. Bulynina, and A. M. Ziganshin, "Influence of granular activated carbon on anaerobic co-digestion of sugar beet pulp and distillers grains with solubles," *Processes*, vol. 8, 2020, doi: 10.3390/pr8101226.

[21] A. A. Pilarska et al., "Additives improving the efficiency of biogas production as an alternative energy source—A review," *Energies*, vol. 17, no. 17, 2024, doi: 10.3390/en17174506.

[22] Q. Li et al., "Biochar and GAC intensify anaerobic phenol degradation via distinctive adsorption and conductive properties," *Journal of Hazardous Materials*, vol. 405, 2021, doi: 10.1016/j.jhazmat.2020.124183.

[23] F. Daneshvar et al., "Critical challenges and advances in the carbon nanotube–metal interface for next-generation electronics," *Nanoscale Advances*, vol. 3, pp. 942–962, 2021, doi: 10.1039/D0NA00822B.

[24] M. J. Sweetman et al., "Activated carbon, carbon nanotubes and graphene: Materials and composites for advanced water purification," *C*, vol. 3, no. 2, 2017, doi: 10.3390/c3020018.

[25] B. Trisakti et al., "Sustainable lipid production from *Chlorella vulgaris* USU1 strain using packed absorption column-derived effluent as carbon source for biomass generation," *Results in Engineering*, vol. 26, 2025, doi: 10.1016/j.rineng. 2025.105383.

[26] F. Zhang et al., "Joint control of multiple food processing contaminants in Maillard reaction: A comprehensive review of health risks and prevention," *Comprehensive Reviews in Food Science and Food Safety*, vol. 24, no. 2, 2025, doi: 10.1111/1541-4337.70138.

[27] T. Selvankumar et al., "Process optimization of biogas energy production from cow dung with alkali pre-treated coffee pulp," *3 Biotech*, vol. 7, 2017, doi: 10.1007/s13205-017-0884-5.

[28] M. Dębowski et al., "Optimisation of biogas production in the co-digestion of pre-hydrodynamically cavitated aerobic granular sludge with waste fats," *Energies*, vol. 17, 2024, doi: 10.3390/en17040922.

[29] T. Torsha and C. N. Mulligan, "Anaerobic treatment of food waste with biogas recirculation under psychrophilic temperature," *Waste*, vol. 2, pp. 58–71, 2024, doi: 10.3390/waste2010003.

[30] M. Szymańska et al., "Anaerobic digestate from biogas plants—Nuisance waste or valuable product?," *Applied Sciences*, vol. 12, 2022, doi: 10.3390/app12084052.

[31] Z. Parsa, R. Dhib, and M. Mehrvar, "Continuous UV/H2O2 process: A sustainable wastewater treatment approach for enhancing the biodegradability of aqueous PVA," *Sustainability*, vol. 16, 2024, doi: 10.3390/su16167060.

[32] L. von Mühlen et al., "Miniaturized method for chemical oxygen demand determination using the PhotoMetrix PRO application," *Molecules*, vol. 27, 2022, doi: 10.3390/su16167060.

[33] R. Ali et al., "BET, FTIR, and Raman characterizations of activated carbon from waste oil fly ash," *Turkish Journal of Chemistry*, vol. 44, 2020, doi: 10.3906/kim-1909-20.

[34] I. Nurhayati et al., "Sustainable pre-treatment of tempeh industry wastewater: Efficiency of vermifiltration in pollutant mitigation and compost production," *Desalination and Water Treatment*, vol. 320, 2024, doi: 10.1016/j.dwt.2024.100820.

[35] I. Utami et al., "Biogas production and removal COD–BOD and TSS from wastewater industrial alcohol (vinasse) by modified UASB bioreactor," *MATEC Web of Conferences*, vol. 58, 2016, doi: 10.1051/matecconf/20165801005.

[36] Y. Li et al., "Effects of organic composition on the anaerobic biodegradability of food waste," *Bioresource Technology*, vol. 243, pp. 836–845, 2017, doi: 10.1016/j.biortech.2017.07.028.

[37] M. R. Pakpahan et al., "Evaluation of wastewater quality of tempeh industry (case study of Tempeh Semanan Industrial Estate)," *AIP Conference Proceedings*, vol. 2646, 2023, doi: 10.1063/5.0117588.

[38] M. Sekine et al., "Improving methane production from food waste by intermittent agitation," *Biomass and Bioenergy*, vol. 164, 2022, doi: 10.1016/j.biombioe.2022.106551.

[39] A. Orangun et al., "Batch anaerobic co-digestion and biochemical methane potential analysis of goat manure and food waste," *Energies*, vol. 14, 2021, doi: 10.3390/en14071952.

[40] S. Muenmee and K. Prasertboonyai, "Potential biogas production generated by mono- and co-digestion of food waste and fruit waste," *Journal of Environmental Engineering and Management*, vol. 77, 2015, doi: 10.5755/j01.erem.77.1.25234.

[41] D. Johnravindar et al., "Supplementing granular activated carbon for enhanced methane production in anaerobic co-digestion of post-consumer substrates," *Biomass and Bioenergy*, vol. 136, 2020, doi: 10.1016/j.biombioe.2020.105543.

[42] A. Calbry-Muzyka et al., "Biogas composition from agricultural sources and organic fraction of municipal solid waste," *Renewable Energy*, vol. 181, pp. 1000–1007, 2022, doi: 10.1016/j.renene.2021.09.100.

[43] M. Pirlou and T. M. Gundoshiman, "The effect of substrate ratio and total solids on methane production," *Journal of Material Cycles and Waste Management*, vol. 23, pp. 1938–1946, 2021, doi: 10.1007/s10163-021-01264-x.

[44] A. Anukam et al., "A review of the chemistry of anaerobic digestion," *Processes*, vol. 7, 2019, doi: 10.3390/pr7080504.

[45] S. Harirchi et al., "Microbiological insights into anaerobic digestion," *Bioengineered*, vol. 13, pp. 6521–6557, 2022, doi: 10.1080/21655979.2022.2035986.

[46] C. Spencer and B. B. Sheff, "Chemistry for digesters," American Biogas Council, Washington, DC, USA, 2017.

[47] A. M. Ali et al., "Production of methane from food waste using anaerobic digestion with biofilm-based pretreatment," *Processes*, vol. 11, 2023, doi: 10.3390/pr11030655.

[48] P. Radadiya et al., "Acidogenic fermentation of food waste in a leachate bed reactor," *Bioresource Technology*, vol. 361, 2022, doi: 10.1016/j.biortech.2022.127705.

[49] M. Michael et al., "Microalgae for sustainable biodiesel and omega-3," *Renewable and Sustainable Energy Reviews*, vol. 226, 2026, doi: 10.1016/j.rser.2025.116327.

[50] H. Feng et al., "Tofu wastewater as a carbon source flowing into municipal wastewater treatment plants," *Journal of Environmental Management*, vol. 370, 2024, doi: 10.1016/j.jenvman.2024.122550.

[51] W. Chen et al., "Granular activated carbon enhances volatile fatty acid production," *Frontiers in Bioengineering and Biotechnology*, vol. 11, 2023, doi: 10.3389/fbioe.2023.1330293.

[52] Q. Jiang et al., "Insight into sludge anaerobic digestion with granular activated carbon

addition," *Bioresource Technology*, vol. 319, 2021, doi: 10.1016/j.biortech.2020.124131.
[53] G. Capson-Tojo et al., "Addition of granular activated carbon and trace elements," *Bioresource Technology*, vol. 260, pp. 157–168, 2018, doi: 10.1016/j.biortech.2018.03.097.
[54] Y. Yang et al., "Adding granular activated carbon into anaerobic sludge digestion," *Journal of Cleaner Production*, vol. 149, pp. 1101–1108, 2017, doi: 10.1016/j.jclepro.2017.02.156.
[55] Y. Xiao et al., "Improved biogas production of dry anaerobic digestion of swine manure," *Bioresource Technology*, vol. 294, 2019, doi: 10.1016/j.biortech.2019.122188.
[56] B. Trisakti et al., "Biogas upgrading via CO2 absorption using monosodium glutamate-promoted potassium carbonate," *South African Journal of Chemical Engineering*, vol. 51, 2025, doi: 10.1016/j.sajce.2024.11.010.
[57] Budiyono et al., "Experiment and modeling to evaluate the effect of total solid on methane production," *Journal of Environmental Studies*, vol. 30, no. 4, pp. 3489–3496, 2020, doi: 10.15244/pjoes/127277.
[58] R. E. Speece, "Anaerobic biotechnology for industrial wastewater treatment," *Environmental Science & Technology*, vol. 17, pp. 324–328, 1983, doi: 10.1021/es00115a725.
[59] A. M. Ritonga et al., "Peningkatan kualitas biogas melalui proses pemurnian," *Jurnal Ilmiah dan Penerapan Keteknikan Pertanian*, vol. 14, no. 1, pp. 1–8, 2021, doi: 10.17969/rtp.v14i1.17321.
[60] N. Azka, "Konstanta pembentukan methane dari limbah cair pabrik kelapa sawit," Skripsi, Universitas Sumatera Utara, Sumatera Utara, Indonesia, 2019.
[61] D. Kalantzis et al., "Granular activated carbon stimulates methane production," *Bioresource Technology*, vol. 376, 2023, doi: 10.1016/j.biortech.2023.128908.
[62] B. Zaman et al., "Utilization of magnetic GAC adsorbent," *IOP Conference Series: Earth and Environmental Science*, vol. 1268, 2023, doi: 10.1088/1755-1315/1268/1/012021.
[63] K. Hussaro et al., "Biogas production from food waste and vegetable waste," *GMSARN International Journal*, vol. 11, 2017.
[64] B. Trisakti et al., "Effect of hydraulic retention time and effluent recycle ratio," *South African Journal of Chemical Engineering*, vol. 50, 2024, doi: 10.1016/j.sajce.2024.08.012.
[65] W. P. Qin and F. Hammes, "Substrate pre-loading influences initial colonization of GAC biofilter biofilms," *Frontiers in Microbiology*, vol. 11, 2020, doi: 10.3389/fmicb.2020.596156.
[66] S. Wang et al., "Comparing the effects and mechanisms of granular activated carbon and magnetite nanoparticles," *Chemical Engineering Journal*, vol. 497, 2024, doi: 10.1016/j.cej.2024.155705.
[67] F. Fazzino et al., "Effects of carbon-based conductive materials on semi-continuous anaerobic co-digestion," *Chemosphere*, vol. 357, 2024, doi: 10.1016/j.chemosphere.2024.142077.
[68] A. Mou et al., "Enhancing methane production from high solid-content wastewater," *Science of the Total Environment*, vol. 906, 2024, doi: 10.1016/j.scitotenv.2023.167609.
[69] Z. Zhang et al., "Enhancing anaerobic digestion and methane production," *Water Research*, vol. 136, pp. 54–63, 2018, doi: 10.1016/j.watres.2018.02.025.
[70] S. Alam et al., "Preparation of activated carbon from the wood of *Paulownia tomentosa*," *Water*, vol. 13, no. 11, 2021, doi: 10.3390/w13111453.
[71] O. Gibert et al., "Characterising biofilm development on granular activated carbon," *Water Research*, vol. 47, no. 3, pp. 1101–1110, 2013, doi: 10.1016/j.watres.2012.11.026.
[72] N. F. Dalimunthe et al., "Pectin-carbonate hydroxyapatite composite films," *Case Studies in Chemical and Environmental Engineering*, vol. 10, 2024, doi: 10.1016/j.cscee.2024.100905.
[73] B. Trisakti et al., "Enhanced H2S absorption and water recovery," *Case Studies in Chemical and Environmental Engineering*, vol. 11, 2025, doi: 10.1016/j.cscee.2025.101173.
[74] X. Yang et al., "Granular activated carbon-driven microbial electron shuttle," *Microbiome*, vol. 13, no. 178, 2025, doi: 10.1186/s40168-025-02161-3.
[75] S. Kalam et al., "Surfactant adsorption isotherms: A review," *ACS Omega*, vol. 6, no. 48, 2021, doi: 10.1021/acsomega.1c04661.
[76] S. Shimizu and N. Matubayasi, "Surface area estimation," *Langmuir*, vol. 38, no. 26, 2022, doi: 10.1021/acs.langmuir.2c00753.
[77] B. Huang et al., "Improved calculations of pore size distribution," *Microporous and Mesoporous Materials*, vol. 184, 2014, doi: 10.1016/j.micromeso.2013.10.008.
[78] S. Fu et al., "Accurate characterization of full pore size distribution," *Energy Science &*

*Engineering*, vol. 9, no. 1, pp. 80–100, 2020, doi: 10.1002/ese3.817.

[79] M. Thommes et al., "Physisorption of gases," *Pure and Applied Chemistry*, vol. 87, 2015, doi: 10.1515/pac-2014-1117.

[80] W. P. Dewi et al., "Variasi penambahan CTABr sebagai template," *Berkala Sainstek*, vol. 7, 2019, doi: 10.19184/bst.v7i2.12857.

[81] L. Feng et al., "Mechanisms, performance, and impact of direct interspecies electron transfer," *Science of the Total Environment*, vol. 862, 2023, doi: 10.1016/j.scitotenv.2022.160813.

[82] R. Sidabutar et al., "Development of a novel co-composting system for empty fruit bunches," *Journal of Hazardous Materials Advances*, vol. 18, 2025, doi: 10.1016/j.hazadv.2025.100730.